

An Overview of the Interatomic Correlation Moments and the Mean Square Relative Atomic Displacements in Anharmonic Crystals

C. G. Rodrigues¹, J. N. Teixeira Rabelo², and V. I. Zubov^{3,4}

¹*Núcleo de Pesquisa em Física, Departamento de Matemática e Física, Universidade Católica de Goiás, Caixa Postal 86, 74605-010 Goiânia, Goiás, Brazil*
²*Instituto de Física, Universidade Federal de Goiás, 74001-970 Goiânia, Goiás, Brazil*
³*Departamento de Física, Universidade Federal de Sergipe, São Cristóvão, Brazil*
⁴*Department of Theoretical Physics, Peoples' Friendship University, Moscow, Russia*

Received on 25 October, 2005

We present an overview of a method developed for the calculation of dynamic interatomic correlations in anharmonic crystals based on the correlative method of unsymmetrized self-consistent field (CUSF). The quadratic correlation momenta and the mean square relative displacements have been calculated for one-, two- and three-dimensional classical models.

Keywords: Lattice dynamics; Correlation moments; Anharmonicity

I. INTRODUCTION

This paper is primarily an extended account of a series of results obtained by the authors in a joint work with other collaborators. The main purpose is to show that on the basis of the Correlative Method of Unsymmetrized Self-consistent Field (CUSF) [1-4] a simple and efficient method is developed to calculate several dynamic properties of highly anharmonic crystals.

In a crystal there are static and dynamic correlations. Of the first type are the correlations between the mean atomic positions. These are very strong and usually called long-range order correlations since they are in intrinsic connection with the localization of each atom in its lattice cell. Of the second type, the short-range ones, are the quadratic correlation moment (QCM) and the mean square relative displacements (MSRD) which express the effective amplitudes of atomic vibrations [5,6]. These quantities hold close relationship to the density fluctuations [7]. The importance of the dynamic correlations is seen in that some melting criteria are defined in terms of the MSRD [8-10].

The QCM and MSRD have been calculated by the dynamical theory of crystal lattices [5,6] but these results are valid only at sufficiently low temperatures [11] because this theory relies upon the harmonic approximation and the account of anharmonicity on its basis by using perturbation theory is rather complicated. Since then, several other approaches have been developed to take into account the anharmonic effects, among which the most prominent is the self-consistent phonon theory [12-21]. In this theory, the harmonic force constants are averaged self-consistently over a trial set of harmonic oscillator functions. For low temperatures, it has faced problems with hard-core potentials that were handled by a more adequate treatment of the short-range correlations instead of using a simple cutoff procedure [19]. It should be mentioned as well the simulation techniques widely used in recent years, especially a Monte Carlo formalism in which the quantum mechanical effects are included by making a modification of the potential energy. This formalism has its origin in a previous illustration by Feynman [22] of the use of the path-integral

form of the partition function in statistical mechanics, and is known as the method of the effective potential and effective Hamiltonian [23-27].

The CUSF [1-4,28-54] method, reported in this review, is free from the hard-core potential problem. More than that, it is just because of the core that the one-particle probability densities vanish except inside the corresponding lattice cell thus leading to a convergence of the statistical averages. It is based on the assumption that the classical phase probability density [55] or the quantum density matrix [31,36,56] is not symmetric with respect to the interchange of coordinates of identical atoms. Here we restrict ourselves to the classical approach. When there is no permutation symmetry, even in the mean-field approximation, which is the zeroth-order one for CUSF, one takes into account the static correlations in crystals (long-range order) and the short-range dynamical correlations preventing the unlimited approach of atoms to each other. Such an approximation includes also the main anharmonic terms of the power-series expansion of the potential energy. Because of this, CUSF provides a good fit to experimental data up to the melting temperatures. The CUSF is applicable not only to perfect, strongly anharmonic crystals, but also to crystals with lattice defects and surfaces [28,29,33-37]. The statistical perturbation theory makes more accurate the contribution of the anharmonicity to thermodynamic functions of crystals, taking into consideration the dynamical interatomic correlations at intermediate and long distances. This enables one to calculate the correlations of the atomic displacements in anharmonic crystals, including strongly anharmonic ones. In section II, we summarize the basic aspects of the method. In section III, we discuss a diagram technique that has been developed in order to make easier the calculation of the perturbation terms. Some applications are shown in section IV and we finish the paper in the section V with a few concluding remarks.

II. GENERAL FORMULAE

In the zeroth approximation of CUSF, the potential energy of a crystal, U , is substituted by a sum of the individual self-

consistent potentials of atoms performing anharmonic vibrations near their lattice points,

$$U^0(\mathbf{r}_1, \mathbf{r}_2, \dots, \mathbf{r}_n) = \sum_{i=1}^N u_i(\mathbf{r}_i). \quad (1)$$

Here, the phase probability distribution is approximated by a product of one-particle probability densities whose configurational parts

$$w_i(\mathbf{r}_i) = \frac{\exp\{-u_i(\mathbf{r}_i)/\Theta\}}{\int \exp\{-u_i(\mathbf{r}_i)/\Theta\} d\mathbf{r}_i} \quad (2)$$

as well as $u_i(\mathbf{r}_i)$ are determined by the basic equations of the unsymmetrized self-consistent field [24-26]; $\Theta = kT$ is the absolute temperature in energy units. Then, the phase probability density in the configurational space is written as

$$w^{(N)}(\mathbf{r}_1, \mathbf{r}_2, \dots, \mathbf{r}_N) = A \exp\{-U'/\Theta\} \prod_{i=1}^N w_i(\mathbf{r}_i), \quad (3)$$

where

$$A^{-1} = \int \exp\{-U'/\Theta\} \prod_{i=1}^N w_i(\mathbf{r}_i) d\mathbf{r}_i. \quad (4)$$

Here,

$$U'(\mathbf{r}_1, \mathbf{r}_2, \dots, \mathbf{r}_N) = U - U^0 \quad (5)$$

is taken as a perturbation. Therefore, when calculating the statistical averages of functions of the atomic coordinates, one can expand (3) and (4) in a power series of U'/Θ .

The MSRД for two atoms i and j in a crystal displacements $\mathbf{q}_i = \mathbf{r}_i - \hat{A}\mathbf{n}_i$ is given by as

$$D_{aa}(ij) = \overline{(q_{ia} - q_{ja})^2} = \overline{q_{ia}^2} + \overline{q_{ja}^2} - 2C_{aa}(ij). \quad (6)$$

Here \hat{A} is the lattice matrix, \mathbf{n}_i are integer-components vectors, a denotes the Cartesian components of atomic displacements and $C_{aa}(ij) = \overline{q_{ia}q_{ja}}$ is the correlation moment. We consider a perfect crystal with pairwise central interactions

$$U(\mathbf{r}_1, \mathbf{r}_2, \dots, \mathbf{r}_N) = \frac{1}{2} \sum_{i \neq j} \Phi(|\mathbf{r}_i - \mathbf{r}_j|). \quad (7)$$

By expanding (1) and (7) in power series of the displacements and retaining anharmonic terms up to fourth order [2,3], the perturbing potential (5) is written in the form

$$U' = U'_2 + U'_3 + U'_4, \quad (8)$$

where

$$U'_2 = -\frac{1}{2} \sum_{i \neq j} \sum_{\alpha, \beta} \Phi_{ij}^{\alpha\beta} q_{i\alpha} q_{j\beta}, \quad (9)$$

$$U'_3 = -\frac{1}{2} \sum_{i \neq j} \sum_{\alpha, \beta, \gamma} \Phi_{ij}^{\alpha\beta\gamma} q_{i\alpha} q_{i\beta} q_{j\gamma}, \quad (10)$$

$$U'_4 = -\sum_{i \neq j} \sum_{\alpha, \beta, \gamma, \delta} \Phi_{ij}^{\alpha\beta\gamma\delta} [q_{i\alpha} q_{i\beta} q_{i\gamma} q_{j\delta} / 6 - (q_{i\alpha} q_{i\beta} q_{j\gamma} q_{j\delta} - q_{i\alpha} q_{i\beta} q_{j\gamma} q_{j\delta}^0 - \overline{q_{i\alpha} q_{i\beta}}^0 \overline{q_{j\gamma} q_{j\delta}}^0) / 8]. \quad (11)$$

The greek letters $\alpha, \beta, \gamma,$ and δ stand for cartesian components, and the zero attached to the bar denotes averaging over the unperturbed distribution, i.e. over (3) when $U' \equiv 0$ and $A = 1$. It can be seen that

$$\overline{q_{i\alpha} q_{j\beta}}^0 = \overline{q_{i\alpha} q_{j\beta}}^0 \delta_{ij}. \quad (12)$$

In Eqs. (9-11) it has been used the notation

$$\Phi_{ij}^{\alpha\beta\dots} = \left[\frac{\partial^{\dots} \Phi|\mathbf{r}|}{\partial x_\alpha \partial x_\beta \dots} \right]_{\mathbf{r}=\hat{A}(\mathbf{n}_i - \mathbf{n}_j)}, \quad (13)$$

for the derivatives of the interatomic potential. All Greek indices are dummy. It follows that: $\overline{U^0} = 0$. Using Eqs. (8-12), we obtain for the variances of the atomic positions [38]

$$\begin{aligned} \overline{q_{ia}^2} = & \overline{a_i^2} + \frac{1}{2\Theta^2} \sum_k \{ \Phi_{\alpha\beta}(ik) \Phi_{\gamma\delta}(ik) \overline{\beta_k \delta_k}^0 \overline{a_i^2 \alpha_i \gamma_i}^0 - \\ & + \overline{a_i^2 \alpha_i \gamma_i}^0 \} + \\ & + \frac{1}{4} \Phi_{\alpha\beta\gamma}(ik) \Phi_{\delta\epsilon\xi}(ik) \overline{\gamma_k \xi_k}^0 \overline{a_i^2 \alpha_i \beta_i \delta_i \epsilon_i}^0 - \\ & - \overline{a_i^2 \alpha_i \beta_i \delta_i \epsilon_i}^0 - 2\overline{\delta_i \epsilon_i}^0 \overline{\gamma_k \xi_k}^0 \overline{a_i^2 \alpha_i \beta_i}^0 - \\ & - \overline{a_i^2 \alpha_i \beta_i}^0 \} + \overline{a_i^2 \alpha_i \delta_i}^0 \\ & - \overline{a_i^2 \alpha_i \delta_i}^0 (\overline{\beta_k \gamma_k \epsilon_k \xi_k}^0 - \overline{\beta_k \gamma_k}^0 \overline{\epsilon_k \xi_k}^0) + \\ & + \frac{1}{3} \Phi_{\alpha\beta}(ik) \Phi_{\gamma\delta\epsilon\xi}(ik) \overline{\beta_k \xi_k}^0 \overline{a_i^2 \alpha_i \gamma_i \delta_i \epsilon_i}^0 - \\ & - \overline{a_i^2 \alpha_i \gamma_i \delta_i \epsilon_i}^0 + \overline{\beta_k \delta_k \epsilon_k \xi_k}^0 \overline{a_i^2 \alpha_i \gamma_i}^0 - \\ & - \overline{a_i^2 \alpha_i \gamma_i}^0 \} \}, \quad (14) \end{aligned}$$

and for the QCM [38]

$$\begin{aligned} C_{ab}(ij) = & \frac{1}{\Theta} \Phi_{\alpha\beta}(ij) \overline{a_i \alpha_i}^0 \overline{b_j \beta_j}^0 + \\ & + \frac{1}{6\Theta} \Phi_{\alpha\beta\gamma\delta}(ij) \overline{a_i \alpha_i \gamma_i \delta_i}^0 \overline{b_j \beta_j}^0 - \\ & - \overline{a_i \alpha_i}^0 \overline{b_j \beta_j \gamma_j \delta_j}^0 + \\ & + \frac{1}{\Theta^2} \sum_k \Phi_{\alpha\gamma}(ik) \Phi_{\beta\delta}(jk) \overline{a_i \alpha_i}^0 \overline{b_j \beta_j}^0 \overline{\gamma_k \delta_k}^0 - \\ & - \frac{1}{4\Theta^2} \Phi_{\alpha\beta\gamma}(ij) \Phi_{\delta\epsilon\xi}(ij) \overline{a_i \alpha_i \gamma_i \delta_i}^0 \overline{b_j \beta_j \epsilon_j \xi_j}^0 + \\ & + \frac{1}{4\Theta^2} \sum_k \Phi_{\alpha\beta\gamma}(ik) \Phi_{\delta\epsilon\xi}(jk) \overline{a_i \alpha_i}^0 \overline{b_j \beta_j}^0 \times \\ & \times (\overline{\beta_k \gamma_k \epsilon_k \xi_k}^0 - \overline{\beta_k \gamma_k}^0 \overline{\epsilon_k \xi_k}^0) + \\ & + \frac{1}{4\Theta^2} \Phi_{\alpha\beta\gamma}(ij) \sum_k (\Phi_{\delta\epsilon\xi}(jk) \overline{a_i \alpha_i}^0 \overline{b_j \beta_j \gamma_j \delta_j}^0 - \\ & - \Phi_{\delta\epsilon\xi}(ik) \overline{b_j \beta_j}^0 \overline{a_i \alpha_i \gamma_i \delta_i}^0) - \\ & - \frac{1}{4\Theta^2} \Phi_{\alpha\beta}(ij) \Phi_{\gamma\delta\epsilon\xi}(ij) \overline{a_i \alpha_i \gamma_i \delta_i}^0 \overline{b_j \beta_j \epsilon_j \xi_j}^0 + \end{aligned}$$

$$\begin{aligned}
 & + \frac{1}{6\Theta^2} \sum_k (\Phi_{\alpha\gamma}(ik) \Phi_{\beta\delta\epsilon\xi}(jk) + \\
 & + \Phi_{\beta\gamma}(jk) \Phi_{\alpha\delta\epsilon\xi}(ik) \overline{a_i \alpha_i^0 b_j \beta_j^0} \overline{\gamma_k \delta_k \epsilon_k \xi_k^0} + \\
 & + \frac{1}{6\Theta^2} \sum_k (\Phi_{\alpha\gamma}(ik) \Phi_{\beta\delta\epsilon\xi}(jk) \overline{a_i \alpha_i^0 b_j \beta_j^0} \overline{\delta_j \epsilon_j} + \\
 & + \Phi_{\beta\gamma}(jk) \Phi_{\alpha\delta\epsilon\xi}(ik) \overline{a_i \alpha_i^0 \delta_i \epsilon_i} \overline{b_j \beta_j^0} \overline{\gamma_k \xi_k^0} \text{ , } (15)
 \end{aligned}$$

In Eqs. (14) and (15) the Latin indices a and b are free, whereas the greek α, β, \dots are dummy. To shorten the expressions in the right-hand side we write a_i, α_i, \dots instead of $q_{ai}, q_{\alpha i}, \dots$. The summation extends over all values k from 1 to N , leaving out i and j . The formulae (14) and (15) are applicable to any Bravais lattice and arbitrary dimensionality.

In the case of a n -dimensional lattice of a high symmetry, these formulae become simpler because only moments of type $\overline{q_\alpha^2}^0$ and $\overline{q_\alpha^2 q_\beta^2}^0$ are nonzero. For a perfect strongly anharmonic crystal, the momenta in the right-hand sides are expressed as [37]

$$\overline{q_\alpha^2}^0 = \frac{\beta_n}{nK_2} \text{ , } (16)$$

$$\overline{q_\alpha^2 q_\beta^2}^0 = (1 + 2\delta_{\alpha\beta}) \left[\frac{6(n - \beta_n)\Theta}{n(n+2)K_4} - \left(\frac{\beta_n\Theta}{nK_2} \right)^2 \right] \text{ , } (17)$$

where $\beta_n(x)$ is the solution of the transcendental equation [37]

$$\beta_n(x) = nx \frac{D_{-(n/2+1)}[x + (n+2)\beta_n/2nx]}{D_{-n/2}[x + (n+2)\beta_n/2nx]} \text{ . } (18)$$

Here $D_\nu(z)$ are the parabolic cylinder functions and x is a dimensionless combination of the temperature and the second- and fourth-order force coefficients $x = K_2 \sqrt{3/\Theta K_2}$ with

$$K_2 = \frac{1}{n} \sum_{\alpha=1}^n K_{\alpha^2} \text{ , } (19)$$

$$K_4 = \frac{3}{n(n+2)} \sum_{\alpha,\beta=1}^n K_{\alpha^2 \beta^2} \text{ , } (20)$$

where

$$K_{\alpha^l \beta^m} = \frac{\partial^{l+m}}{\partial q_\alpha^l \partial q_\beta^m} \sum_{\mathbf{n} \neq 0} \Phi(|\mathbf{q} - \hat{\mathbf{A}}\mathbf{n}|) |_{\mathbf{q}=0} \text{ . } (21)$$

The lattice matrix $\hat{\mathbf{A}}$ can be calculated from the equation of state. In the case of a n -dimensional lattice of high symmetry with strong anharmonicity up to the fourth order under hydrostatic pressure the equation of state is [37]

$$\begin{aligned}
 P = & - \frac{a}{nv_n(a)} \left(\frac{1}{2} \frac{dK_0}{da} + \frac{\beta_n\Theta}{2K_2} \frac{dK_2}{da} + \frac{(n - \beta_n)\Theta}{4K_4} \frac{dK_4}{da} \right) + \\
 & + P^2 + P^H + P^Q \text{ . } (22)
 \end{aligned}$$

Here, a is the nearest neighbor distance, $v_n(a)$ is the volume of the unit cell and $K_0(a)/2$ is the energy per molecule in the static lattice; P^Q is the first quantum correction and P^2 and P^H are the corrections provided by the perturbation theory which refine contributions of the anharmonic terms to thermodynamic properties. At constant pressure, this equation with various interatomic potentials has two roots $a_1(T) \leq a_2(T)$ up to some limiting temperature T_S where $a_1(T_S) = a_2(T_S)$ and the isothermal bulk modulus is equal to zero [28,30,41,44,47]. At high temperatures, Eq. (22) has no real roots. For van der Waals crystals at normal pressure its instability temperature (spinodal point) T_S is about 1.35 times greater than its melting point T_m . We have calculated QCM and MSRD along the lower branch of the normal isobar which represents the stable thermodynamic states.

The expressions (16) to (21) are valid for strongly anharmonic crystals. When the anharmonicity is weak, i.e. the temperature is not very high,

$$\beta_n \approx n[1 - (n+2)/x^2]; \quad x \gg 1 \text{ . } (23)$$

III. DIAGRAM TECHNIQUE

With each term in the right-hand side of Eqs. (14) and (15), we properly associate a diagram. We next formulate the rules for drawing them. Each diagram consists of vertices connected by one or several lines with bars. Some of the vertices have besides the lines branches ending in a bar. The total number of lines is equal to the order of the perturbation theory. Each vertex corresponds to an atom in a lattice point and represents the momenta of a one-particle function such as Eqs. (16) and (17). The order of a moment is equal to the number of bars near the vertex. The line denotes the derivatives of the interatomic potential [Eq. (13)] whose order is equal to the number of bars on this line. The branches with bars correspond to the displacements of the atoms whose moments are calculated. In the general case, summation is carried out over the cartesian components. The vertices with branches tally the fixed lattice points, whereas other vertices are dummy.

These diagrams, like those known diagrams introduced by Feynman and Mayer, can be connected or disconnected. The contribution of each disconnected diagram is proportional to N^{l-1} , where l is the number of its connected parts. All such contributions cancel each other. Expression (15) contains only connected diagrams.

In Fig. 1, the diagrams are represented in the same sequence as in Eq. (15). One can see the physical meaning of each term in Eq. (15). The first and third diagrams express the correlation momenta in the harmonic approximation and the others take into account the anharmonicity. The diagrams A, B, D and G correspond to those parts of correlations between two atoms that are due to their mutual interactions. Those parts of their correlations which are represented by the diagrams C, E, H and I are caused by the interactions of both of them with other (intermediate) atoms. At last, the diagram F takes into account the influence of the surrounding atoms (background) on the first part of the correlations, which is brought about by the anharmonicity.

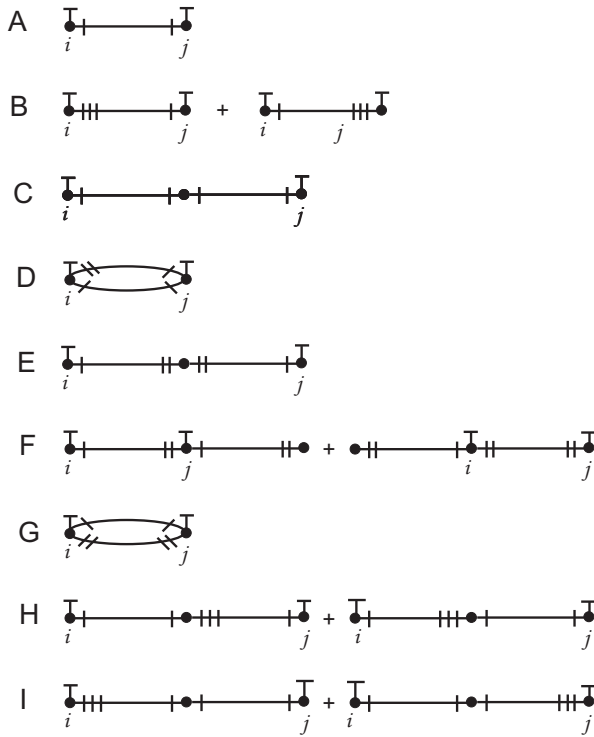


FIG. 1: Diagrams for Eq. (15). Only vertices corresponding to fixed lattice points are indexed.

One may notice that similar diagrams can be used to obtain corrections to the Helmholtz free energy of strongly anharmonicity crystal [34]. However, in that case there are no vertices with branches.

For the variances of the atomic position [Eq. (14)] the diagrams are drawn as it has been done for the interatomic correlations. Each of them, representing an additional influence (i.e. not included in the zeroth approximation [Eq. (16) and (17)]) of the vibrations of neighbors on the momenta of the displacement of the given atom, contains the vertices and the inner and outer lines with bars, as shown in Fig. 2.

IV. APPLICATIONS

A. One-dimensional model: linear chain

As a first application of these general results, we study firstly a monatomic linear chain (see Fig. 3). In these calculations we have used the Morse interatomic potential (see Appendix).

In Fig. 4, we compare MSR in a linear chain using various approximations, taking the relative displacements between the next to nearest neighbors. Data of the weakly anharmonicity approximation are close to those of the strongly anharmonic approximation. At very low temperatures all values practically coincide. However, at high temperatures the differences between results of strongly anharmonic computations and those of harmonic and weakly anharmonic approxima-

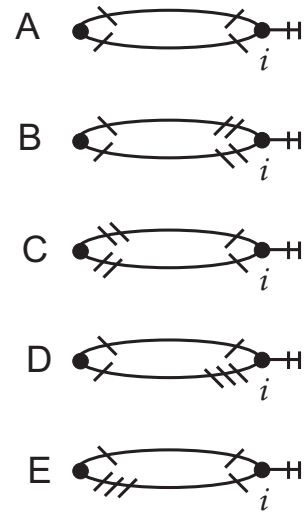


FIG. 2: All diagrams for Eq. (14).

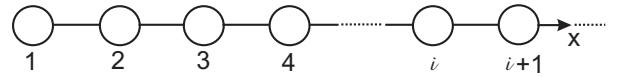


FIG. 3: A monoatomic linear chain.

tions reach about 40 and 11% respectively. For the nearest and third neighbors, the results of various approaches can show the important role of anharmonic effects at high temperatures [38,39].

MSRD between nearest, second, and third neighbors in linear chain are represented in Fig. 5 taking into account the strong anharmonicity of their vibrations. As one should ex-

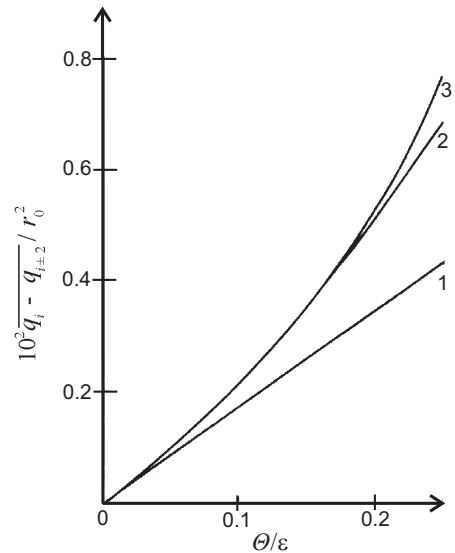


FIG. 4: MSR between the next-nearest neighbors in various approximations: (1) harmonic, (2) weakly anharmonicity, and (3) strongly anharmonic.

pect, MSRD increases with interatomic distance [38,39].

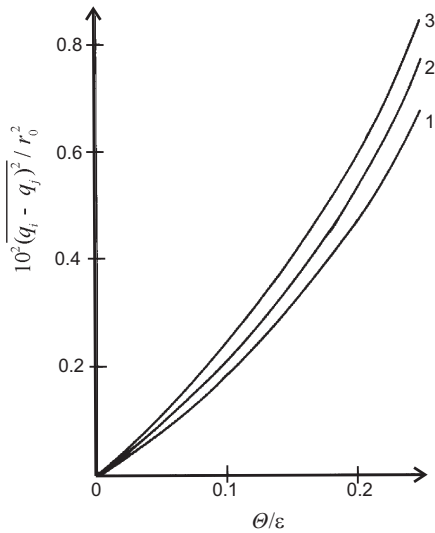


FIG. 5: MSRD between various neighbors taking into account the strong anharmonicity: (1) nearest, (2) second, (3) third neighbors.

B. Two-dimensional models: square and hexagonal lattices

Here, we investigate QCM and MSRD in some two-dimensional models of a weakly anharmonic crystal with square [40,43] and hexagonal lattices [44], using for the numerical evaluations the Morse potential which is typical for short-range interactions. In the two-dimensional case only the square and hexagonal lattices are compatible with pairwise central forces.

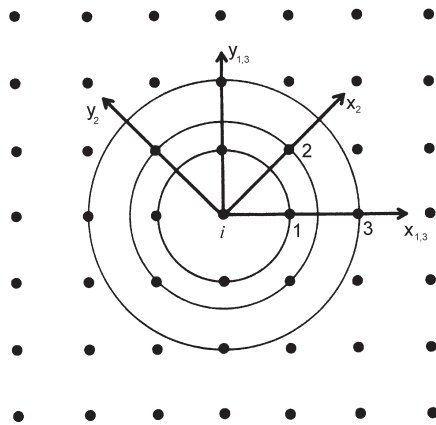


FIG. 6: A fragment of the square lattice with the coordinate systems for the nearest, second and third neighbors.

In Fig. 6 there are shown three coordination circles of the fragment of a two-dimensional model with square lattice. We calculate the QCM and MSRD of the atomic displacements of the nearest and third neighbors in the coordinate system

$X_{1,3} \times Y_{1,3}$, and for second neighbors the system $X_2 \times Y_2$ (see Fig. 6). In the coordinate system used, $C_{xy}(k) = 0$. In Fig. 7 we represented the longitudinal components of MSRD for the square lattice. For the nearest neighbors the harmonic approximation is also shown to demonstrate the anharmonic effects which are appreciable here. One can see that $D_{xx}(1)$ and $D_{xx}(3)$ are very close to MSRD between the nearest and second neighbors in the weakly anharmonic one-dimensional model. This behavior is peculiar only to square and simple cubic lattices owing to right angles between interatomic bonds.

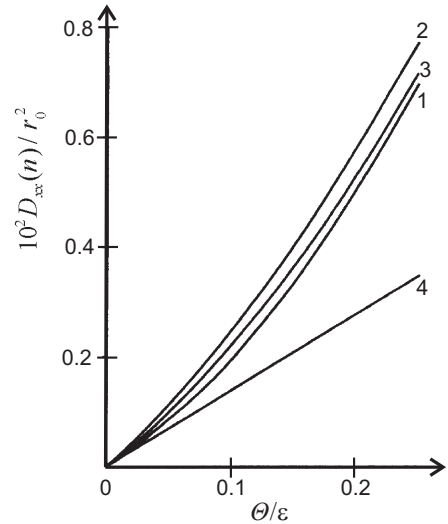


FIG. 7: Longitudinal components of MSRD, in square lattice, between the first (1), second (2), and third (3) neighbor, (4) the harmonic approximation for $D_{xx}(1)$.

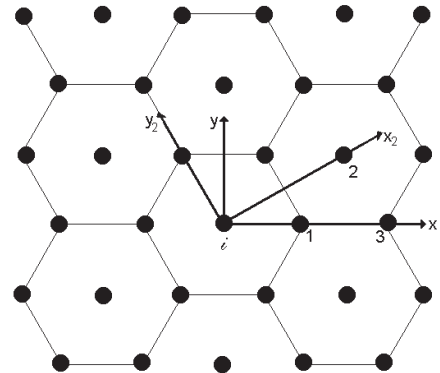


FIG. 8: A fragment of the hexagonal lattice with the coordinate systems for the nearest, second and third neighbors.

The two-dimensional hexagonal lattice represented in Fig. 8 is the simplest model of a close-packed crystal. For any pair of atoms, we shall use the coordinate system whose X -axis runs through the corresponding lattice points. In the case of second neighbors, the axes are denoted by $X_2 \times Y_2$ in Fig. 8. In such systems, $C_{xy}(k) = 0$. Basically, the correlations between the longitudinal atomic displacements, in hexagonal

lattice, are smaller and correlations between transversal displacements are larger than those in the square lattice [40]. The exceptions are $C_{xx}(2)$ and $C_{yy}(3)$. It is interesting that transversal correlations between the second and third neighbors are negative. For an atomic pair $|C_{yy}(k)| < C_{xx}(k)$. In the harmonic approximation $C_{yy}^h(1) = C_{xx}^h(2) = -3C_{yy}^h(3)$. Anharmonic effects violate these simple relations. QCM decreases as the interatomic distance increases, with it going slower along the line passing through a nearest neighbor of an atom than along other directions. Some results are presented in Fig. 9.

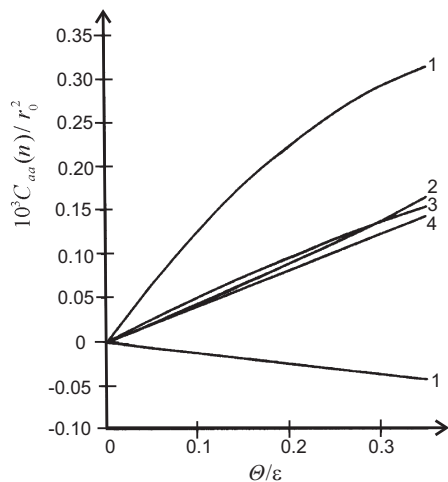


FIG. 9: Quadratic correlations moments in hexagonal lattice: 1- $C_{xx}(1)$, 2- $C_{yy}(1)$, 3- $C_{xx}(3)$, 4- $C_{xx}(2)$, 5- $C_{yy}(2)$.

In the hexagonal lattice, the QCM and MSRD are, for the most part, less than those in the linear chain [38,39] and in the square lattice [40,43]. The exception is the case of correlations between the second neighbors in the latter. Anomalous (very small) magnitudes of the correlations between the second neighbors in the square lattice are caused by right angles between interatomic bonds, and appear to be associated with the instability of such lattice relative to shearing strain when only the nearest neighbors interact.

C. Three-dimensional models: the cubic lattices

1. Simple cubic lattice

In Fig. 10, we show a fragment of a simple cubic lattice (sc) with the coordinate systems. Here we have used the Morse potential to calculate QCM and MSRD. For any pair of atoms, we use the coordinate system whose X -axis runs through the corresponding lattice points. To calculate the QCM for the nearest, and fourth neighbors, we considered here the crystallographic coordinate system $X \times Y$ as shown in Fig. 10. To make easier the calculations of the correlation momenta of the second neighbor displacements we have chosen the axes denoted as X_2, Y_2 in Fig. 10. In this model, the QCM between

the third neighbors vanishes in the second order of perturbation theory.

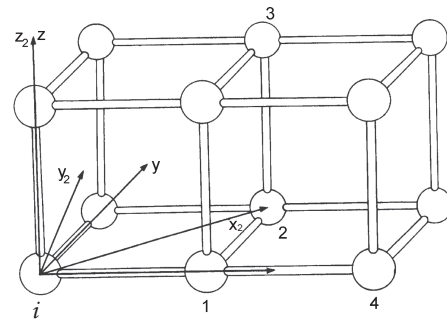


FIG. 10: A fragment of a simple cubic lattice with the coordinate system.

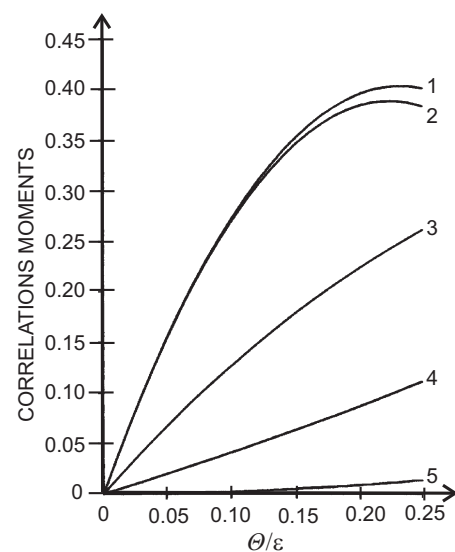


FIG. 11: Comparison of quadratic correlation moments, $10^3 C_{\alpha\alpha}(k)/r_0^2$, between the nearest neighbors in various lattices: 1- $C_{xx}(1)$ in a simple cubic lattice, 2- $C_{xx}(1)$ in a square lattice, 3- $C_{xx}(1)$ and 4- $C_{yy}(1)$ in a hexagonal lattice, 5- $C_{yy}(1)$ in a simple cubic and square lattices.

In Fig. 11, we compare the correlations versus dimensionless temperature Θ/ϵ plot for the sc crystal with those in two-dimensional models with square and hexagonal lattices. Note that the magnitudes of the longitudinal and transversal components of QCM for the square and sc lattices are very close. It is seen that the longitudinal components for the nearest neighbors are larger and the transversal components are smaller than those in an hexagonal lattice. However, the magnitudes of the longitudinal and transversal components of correlations for the second neighbors are smaller than those of the longitudinal components and larger than those of the transversal components of QCM in a hexagonal lattice. This behavior is so because QCM is dependent on the dimensionality of the lattice and the coordination number [45].

In Fig. 12, we compare the longitudinal components of

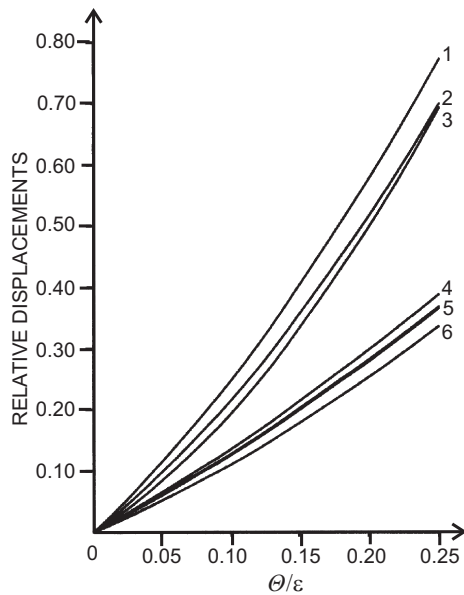


FIG. 12: Mean square displacements, $100D_{\alpha\alpha}(k)/r_0^2$: 1- $D_{\alpha\alpha}(k)$ where $k \geq 4$, 2- $D_{xx}(4)$, 3- $D_{xx}(1)$ in a simple cubic lattice, and 4- $D_{\alpha\alpha}(k)$ where $k = 3, 5, 6, 7, \dots$, 5- $D_{xx}(2) \simeq D_{xx}(3)$, 6- $D_{xx}(1)$ in a hexagonal lattice.

MSRD in a sc lattice with those in an hexagonal lattice. One can see that the mean square relative displacements of the latter are smaller than those in the former. Note that the first and second neighbors in a sc lattice are similar to the first and second neighbors respectively in the square lattice and in the linear chain. Moreover, the fourth neighbors in a sc lattice correspond to the third neighbors in a square lattice [46].

Basically, the correlation momenta between the longitudinal ($a = x$) displacements are larger and the correlations between the transversal ones ($a = y, z$), and are smaller for the sc lattice than those for low-dimensional models.

2. Face-centered cubic lattice

We consider now the fcc crystal in which only nearest neighbors interact. Such a lattice is represented in Fig. 13, where the X -axis for various pairs of atoms are shown and a fragment of a close-packed (111) plane is shaded.

In Fig. 14, we compare the correlations and the variances of the atomic positions for the fcc, sc and two-dimensional hexagonal lattices, using the Morse potential. The temperature $\Theta/\epsilon = 0.5$ is close to the melting point of the fcc crystal with nearest-neighbor interactions. Temperature intervals for other models have been chosen by having in mind that their melting points must be proportional to their coordination numbers. The same qualitative remarks made in the first-order perturbation theory remain valid in the second-order: (i) the more is the coordination number in a lattice the less is the lengthwise correlation between the nearest neighbors; (ii) in the case of close-packed lattices, these values decrease with increasing dimensionality [47].

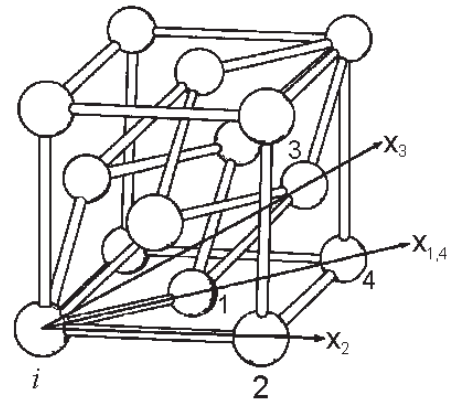


FIG. 13: The spatial arrangement of the neighbors of an atom in the fcc lattice.

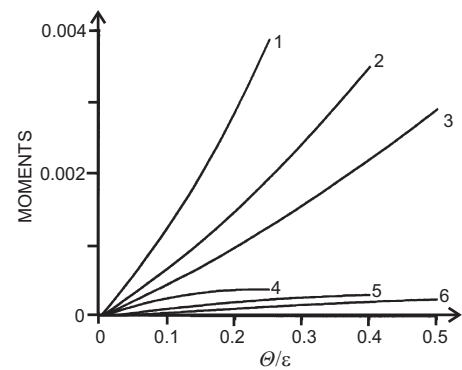


FIG. 14: Variances of the atomic positions $\overline{q_{\alpha}^2}/r_0^2$ (1-3) and lengthwise correlations between the nearest neighbors $C_{xx}(1)/r_0^2$ (4-6) versus dimensionless temperature Θ/ϵ in the simple cubic (1,4), two-dimensional hexagonal (2,5) and face-centered cubic (3,6) weakly anharmonic lattices.

In Fig. 15, results for the longitudinal correlation moment between the nearest neighbors $C_{xx}(1)$, calculated with the account of strong anharmonicity, are compared with those obtained in the harmonic and weakly anharmonic approximations. We have used this time the Lennard-Jones potential. It is seen that only at very low temperatures ($T < 0.4T_m$) all the three curves are very close to one another, and at high temperatures the moment in the weakly anharmonic approximation decreases with increasing temperature. The strong anharmonicity leads to a change in the convexity and a sharp enhancement of $C_{xx}(1)$ near the melting temperature, in the metastable region $T_m < T < T_S$ and especially when $T \rightarrow T_S$. As this takes place, the strong anharmonicity significantly affects the interatomic correlations. It can be noticed as well that a drastic rise in $C_{xx}(1)$, in the vicinity of T_S , corresponds to the general concept about the behavior of fluctuations and correlations of physical quantities near the spinodal [52].

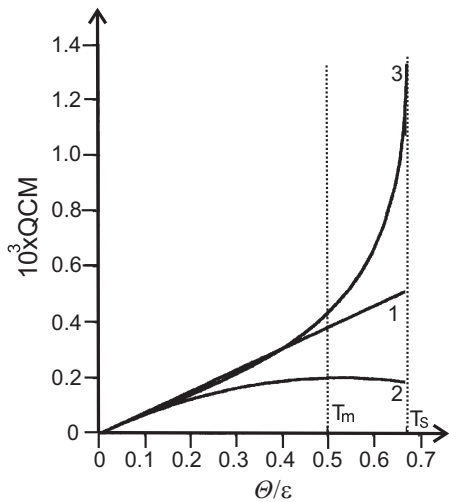


FIG. 15: Quadratic correlations moments between longitudinal displacements of the nearest neighbors calculated using various approximations: (1) harmonic, (2) weakly anharmonic, (3) strongly anharmonic.

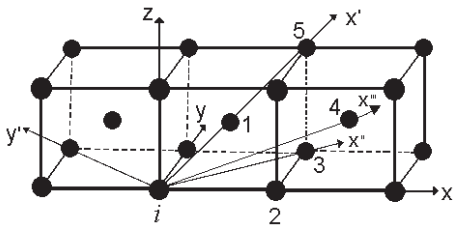


FIG. 16: The arrangement of the neighbors of an atom in the bcc lattice for the spatial fragment of this lattice.

3. Body-centered cubic lattice

A spatial fragment of a strongly anharmonic crystal with body centered lattice (bcc) is shown in Fig. 16. In this case, we can see from formula (15) that the second-order perturbation theory yields the calculation of the momenta including up to the fifth neighbors. For the second neighbors, it is more convenient to use the crystallographic coordinate system. Finally, with a rotation of $\pi/4$ around the crystallographic Z-axis, we obtain the correlation momenta between the third neighbors. Here, we used the Schiff and the Lennard-Jones potentials for the numerical evaluations (see Appendix).

In Fig. 17, we have compared the longitudinal correlation momenta calculated using the Lennard-Jones and Schiff potentials. We can see that the correlation momenta using the Schiff potentials for Na are less anharmonic and at high temperatures their values are also less than the ones calculated by the Lennard-Jones potential with the exception of the curves $C_{xx}(5)$ and $C_{yy}(1)$. The melting temperature of Na is 373 K. For temperatures less than 50 K, Na has another crystal structure. For this reason, we investigated the QCM and MSRD in the temperature range between 50 K and 373 K [49,52]. It is seen that some momenta are negative, implying that the

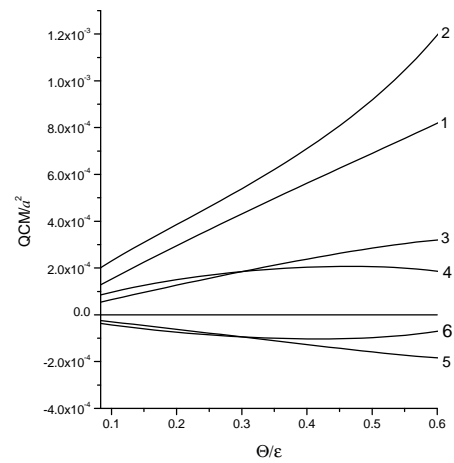


FIG. 17: Longitudinal correlations moments $C_{xx}(1)-(1,2)$, $C_{xx}(1)-(3,4)$ and $C_{xx}(2)-(5,6)$ calculated using the Schiff (1,3,5) and the Lennard-Jones (2,4,6) potentials.

corresponding atoms oscillate in such a direction for the most part opposite in phase. The negative sign of the longitudinal correlation moment in the second-order perturbation theory is because of an obtuse angle between them and each of their common nearest neighbor. When this angle is acute, such a correlation is positive and in the case of a straight angle, it is very small being proportional to the squared temperature. Due to the symmetry of the coordinate systems, the components of transversal correlations between the nearest, second and fifth neighbors are the same, namely $C_{yy}(n) = C_{zz}(n)$, $n = 1, 2, 5$. It can be noticed that the transversal correlations are much smaller than the longitudinal ones.

4. C_{60} fullerite

The method was applied also to C_{60} fullerites, using an intermolecular potential proposed by Girifalco (see appendix). In Fig. 18, we show the X-axis for various molecular pairs and also other axes for the second neighbors. In Fig. 19, a comparison is shown of the QCM longitudinal and transversal components between the fullerite and the solid Ar [53]. The qualitative agreement is because both materials have the fcc crystal lattice with short-range interactions. But C_{60} values are by far smaller than those for Ar. For instance, at 1500 K, that has been evaluated as the triple point temperature [47] the Lindemann parameter is about 0.041, which is less than for Ar by a factor of 1.9 – 2.4.

The melting curve of this fullerite was estimated [54]. To do this, the equation of state was solved at various fixed pressures up to the temperature $T_m(P)$, at which the Lindemann parameter is equal to 0.041 and the molar volume was calculated at this melting point $V = V_m(P)$. The results are shown in Fig. 20. The melting curve was calculated from the melting point at normal pressure, estimated at 1500 K up to 15 kbar corresponding to a melting temperature $T_m = 4000$ K.

The liquid phase of fullerites has never been observed.

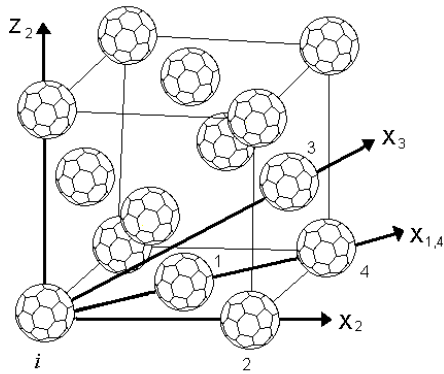


FIG. 18: The arrangement (a spatial fragment) of the neighbors of a molecule in the high-temperature modification of C_{60} fullerite with the coordinate axis for various molecular pairs

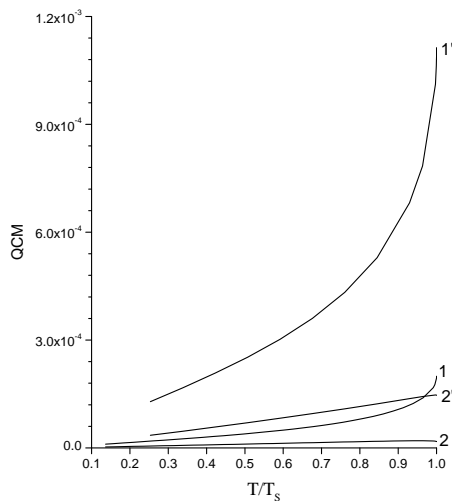


FIG. 19: QCM in a C_{60} fullerite (1,2) and in a solid Ar (1', 2')(1,1') $C_{xx}(1)$, (2,2') $C_{yy}(1)$

Nevertheless, discussion about its possible existence has persisted for years, based on a cluster-expansion-type method [58], an integral-equation approach [59], a Monte Carlo technique [60,61,62], a density-functional theory [62,63], molecular dynamics simulations [58,64], a modified hypernetted-chain method [66] and also on the scaling of Lennard-Jones values [59].

The temperature dependence of the melting pressure is very well described by the Simon equation

$$\frac{(P_m(T)/\text{bar}) - 1}{b} = \left(\frac{T}{T_0}\right)^c, \quad (24)$$

where $T_0 = 1500$ K, $b = 6643.8$ and $c = 1.209$. The temperature dependence of the molar volume along the melting curve is approximated by [55]

$$V_s(T) = V_s(T_0) - 29.20 \ln(T/T_0), \quad (25)$$

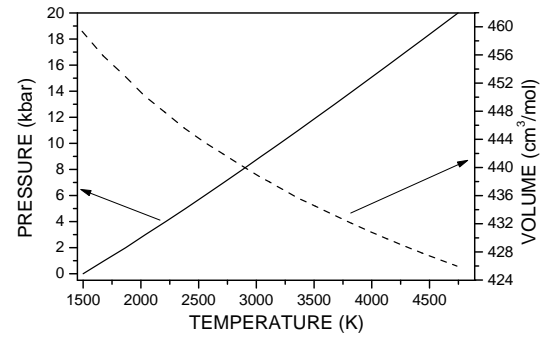


FIG. 20: The possible melting curve of C_{60} fullerite

V. CONCLUDING REMARKS

In summary, a method is given for the calculation of interatomic correlations in anharmonic crystals. We have given here a classical approach, although it enables also the calculation of quantum correction [31]. When there is no permutation symmetry, even in the zeroth mean-field approximation, the long-range static and the short-range dynamic correlations are taken into account preventing the unlimited approaching of atoms to each other. Such an approximation includes also the main anharmonic terms of the power series expression of the potential energy. Corrections calculated by statistical mechanical perturbation theory improve the zeroth-order approximation making more accurate the account of the anharmonicity in the thermodynamical functions of crystals and also including the calculations at intermediate and long distances.

We note that CUSF yields good results for thermodynamic properties of strongly anharmonic crystals with various lattices and bonds: for van der Waals crystals [28,42], ionic crystals [30], fullerites [54,55] and also for Sodium [41,50,52] based on an effective interionic potential [58]. The CUSF is applicable not only to perfect, strongly anharmonic crystals, but also to crystals with lattice defects and surfaces as well [29,33-36], allowing to study structural, dynamical and thermodynamical properties and providing a good agreements to available experimental data up to the melting temperatures [55].

APPENDIX A: POTENTIALS

In this work we used the potentials:

1. Morse potential

The Morse interatomic potential is

$$\Phi(r) = \varepsilon [e^{-2\rho(r-r_0)} - 2e^{-\rho(r-r_0)}], \quad (A1)$$

where $\rho = 6/r_0$, being ε the depth of the potential and r_0 is the minimum point of the interatomic potential.

2. Lennard-Jones potential

The Lennard-Jones potential

$$\Phi(r) = 4\epsilon \left[\left(\frac{\sigma}{r} \right)^{12} - \left(\frac{\sigma}{r} \right)^6 \right], \quad (\text{A2})$$

where $\sigma = r_0/2^{1/6}$. The latter potential is more anharmonic and decreases with increasing interatomic distances somewhat slower than former.

3. Schiff potential

Schiff [67] proposed the following potential for Sodium which is a typical crystal with the bcc lattice

$$\begin{aligned} \Phi(r) = & \epsilon \left(A + B/R^2 + C/R^4 \right) \frac{\cos(2k_F R)}{R^3} + \\ & + \epsilon \left(D + E/R^2 \right) \frac{\sin(2k_F R)}{R^4}, \end{aligned} \quad (\text{A3})$$

where $R = r/\sigma_{eff}$, is the depth of the potential $\epsilon/k = 599K$, $\sigma_{eff} = 0.324$ nm the effective diameter of an ion screened by

free electrons. The parameters are: $A = 0.19$, $B = -1.02$, $C = -0.08$, $D = -0.43$, $E = -2.54$, $2k_F = 5.987$. Such potential is of an oscillating form, what is known as Friedel oscillations. Essentially all calculations that use such potentials refer to numerical modeling [68].

4. Girifalco potential

The potential proposed by Girifalco [69] for the fullerenes has the form

$$\begin{aligned} \Phi(r) = & -\alpha \left(\frac{1}{s(s-1)^3} + \frac{1}{s(s+1)^3} - \frac{2}{s^4} \right) + \\ & + \beta \left(\frac{1}{s(s-1)^9} + \frac{1}{s(s+1)^9} - \frac{2}{s^{10}} \right), \end{aligned} \quad (\text{A4})$$

where $s = r/2a$, $a = 3.55 \times 10^{-8}$ cm, $\alpha = 7.494 \times 10^{-14}$ erg and $\beta = 1.3595 \times 10^{-16}$ erg. Its minimum point is is $r_0 = 10.0558$ Å and the well depth is $\epsilon/k = 3218.4$ K. A method was proposed in [70] for the calculation of the coefficients of this potential for a series of smaller and higher fullerenes, from the C_{28} to the C_{96} (see also [71,72]).

-
- [1] V.I. Zubov, Y.P. Terletskii, Ann. Phys. (Leipzig) **24**, 97 (1970).
 [2] V.I. Zubov, Ann. Phys. (Leipzig) **31**, 33 (1974).
 [3] V.I. Zubov, Phys. Stat. Sol. (b) **72**, 71, 483 (1975).
 [4] V.I. Zubov, Phys. Stat. Sol. (b) **87**, 385 (1978);
 [5] M. Born, K. Huang, *Dynamical theory of crystal lattices* (Clareidon Press (1954)).
 [6] G. Leibfried, *Gittertheorie der mechanischen and thermischen eigenschaften der kristalle* (Springer, Berlin, 1955).
 [7] V.I. Yukalov, Physica A **213**, 500 (1995).
 [8] Zheng-Hua Fang, J. Phys.: Cond. Mat. **8**, 7067 (1996).
 [9] M. Ross, Phys. Rev. B **184**, 233 (1969).
 [10] S. M. Stishov, Uspekhi Fiz. Nauk, **114**, 3 (1974).
 [11] M. L. Klein, G. K. Horton, J. Low Temp. Phys. **9**, 151 97 (1970).
 [12] D. J. Hooton, Phil. Mag. **3**, 49 (1958).
 [13] L. H. Nosanow, Phys. Rev. **146**, 12 (1966).
 [14] Ph. Choquard, *The Anharmonic Crystal*, (W.A. Benjamin, New York 1967).
 [15] H. Horner, Z. Phys. **205**, 72 (1967).
 [16] W. Götze, K.H. Michel, Z. Phys. **217**, 170 (1968).
 [17] N.M. Plakida, T. Siklós, Phys. Stat. Sol. (b) **33**, 103; 113 (1969).
 [18] N.M. Plakida, T. Siklós, Phys. Stat. Sol. (b) **39**, 171 (1970).
 [19] H. Horner, Solid State Commun. **9**, 79 (1971).
 [20] M.L. Klein, G.K. Horton, J. Low-Temp. Phys. **9**, 151 (1972).
 [21] N.M. Plakida, T. Siklós, Acta Phys. Hungar. **45**, 37 (1978).
 [22] R.P. Feynman, *Statistical mechanics*, (Reading, MA: Benjamin, 1972).
 [23] R. Giachetti, V. Tognetti, Phys. Rev. Lett. **55**, 912 (1985)
 [24] R. Giachetti, V. Tognetti, Phys. Rev. B **33**, 7647 (1986).
 [25] R.P. Feynman, H. Kleinert, Phys. Rev. A **34**, 5080 (1986).
 [26] V.B. Magalinskii, Sov. Phys. JETP, **72**, 103 (1991).
 [27] A. Cuccoli, R. Giachetti, V. Tognetti, R. Vaia, and P. Verrucchi, J. Phys.: Condens. Matter **7**, 7891 (1995).
 [28] V.I. Zubov, Phys. Stat. Sol. (b) **101**, 95 (1980).
 [29] V.I. Zubov, Phys. Stat. Sol. (b) **111**, 417 (1982).
 [30] V.I. Zubov, S.S. Soulayman, Kristallografia **27**, 588 (1982), in Russian.
 [31] V.I. Yukalov, V.I. Zubov, Fortschr. Phys. **31**, 627 (1983).
 [32] V.I. Zubov, M.F. Pascual, Izv. vuzov (Tomsk) Fiz. no. 6, 67 (1984).
 [33] V.I. Zubov, J.N. Rabelo, Phys. Stat. Sol. (b) **138**, 433 (1986).
 [34] V.I. Zubov, F. Banyeretse, N.P. Tretyakov, and I.V. Mamontov, Internat. J. Mod. Phys. B **4**, 317, 479 (1990).
 [35] V.I. Zubov, N.P. Tretyakov, Phys. Stat. Sol. (b) **164**, 409 (1991)
 [36] V.I. Zubov, Internat. J. Mod. Phys. B **6**, 367 (1992).
 [37] V.I. Zubov, I.V. Mamontov, and N.P. Tretyakov, Internat. J. Mod. Phys. B **6**, 197, 221 (1992).
 [38] V.I. Zubov, M.F. Pascual, and J.N.T. Rabelo, Phys. Stat. Sol. (b) **175**, 331 (1993).
 [39] V.I. Zubov, M.F. Pascual, J.N.T. Rabelo, and A.C. Faria, Phys. Stat. Sol. (b) **182**, 315 (1994).
 [40] V.I. Zubov, M.F. Pascual, Mod. Phys. Lett. B **8**, 523 (1994).
 [41] J.F.S. Ortiz, N.P. Tretyakov, and V.I. Zubov, Phys. Stat. Sol. (b) **181**, K7 (1994).
 [42] V.I. Zubov, N.P. Tretyakov, and J.F. Sanchez, Internat. J. Mod. Phys. B **9**, 3559 (1995).
 [43] M.F. Pascual, V.I. Zubov, Mod. Phys. Lett. B **9**, 1513 (1995).
 [44] V.I. Zubov, M.F. Pascual, and C.G. Rodrigues, Mod. Phys. Lett. B **9**, 839 (1995).

- [45] V.I. Zubov, N.P. Tretiakov, J.F. Sanchez, and A.A. Caparica, Phys. Rev. B **53**, 12080 (1996).
- [46] M.F. Pascual, A.L. Rosa, and V.I. Zubov, Mod. Phys. Lett. B **10**, 599 (1996).
- [47] V.I. Zubov, M.F. Pascual, and C.G. Rodrigues, Mod. Phys. Lett. B **10**, 1043 (1996).
- [48] V.I. Zubov, J.F. Sanchez-Ortiz, and J.N.T. Rabelo, Phys. Rev. B **55**, 6747 (1997).
- [49] C.G. Rodrigues, M.F. Pascual, and V.I. Zubov, Braz. J. Phys. **27**, 448 (1997).
- [50] J.F.S. Ortiz, N.P. Tretiakov, and V.I. Zubov, Phys. Stat. Sol. (b) **200**, 27 (1997).
- [51] V.I. Zubov, C.G. Rodrigues, and M.F. Pascual, Internat. J. Mod. Phys. B **12**, 2869 (1998).
- [52] C.G. Rodrigues, V.I. Zubov, and M.F. Pascual, Braz. J. Phys. **29**, 450 (1999).
- [53] V.I. Zubov, C.G. Rodrigues, Phys. Stat. Sol. (b) **222**, 471 (2000).
- [54] V.I. Zubov, C.G. Rodrigues, and I.V. Zubov, Phys. Stat. Sol. (b) **238**, 110 (2003).
- [55] C.G. Rodrigues, Czech. J. Phys. **54**, 849 (2004).
- [56] Y.P. Terletskii, *Statistical physics*, (North-Holland Publ. Co., Amsterdam, 1971).
- [57] A. Messiah, *Quantum Mechanics*, (North-Holland Publ. Co., Amsterdam, 1961).
- [58] N.W. Ashcroft, Europhys. Lett. **16**, 355 (1991); Nature **365**, 387 (1993).
- [59] A. Cheng, M.L. Klein, and C. Caccamo, Phys. Rev. Lett. **71**, 1200 (1993).
- [60] M.H.J. Hagen, E.J. Meijer, G.C.A.M. Mooij, D. Frenkel, and H.N.W. Lekkerkerker, Nature **365**, 425 (1993).
- [61] M. Hasegawa, J. Chem. Phys. **111**, 5955 (1999).
- [62] M. Hasegawa, K. Ohno, J. Chem. Phys. **113**, 4315 (2000).
- [63] L. Mederos, G. Navasqués, Phys. Rev. B **50**, 1301 (1994).
- [64] M. Hasegawa, K. Ohno, Phys. Rev. E **54**, 3928 (1996).
- [65] M.A. Abramo, G. Coppolino, Phys. Rev. B **58**, 2372 (1998).
- [66] C. Caccamo, Phys. Rev. B **51**, 3387 (1995).
- [67] D. Schiff, Phys. Rev. **186**, 151 (1969).
- [68] A.E. Galashev, *Teplofizicheskie svoistva metastabilnikh sistem*, (Academy of Sciences of USSR, p. 35, 1984) (in Russian).
- [69] L.F. Girifalco, J. Phys. Chem. **96**, 858 (1992).
- [70] V.I. Zubov, Mol. Mater. **13**, 385 (2000).
- [71] V.I. Zubov, Internet Electron. J. Nanociencia et Moletronica, **2**, 249 (2004).
- [72] V.I. Zubov, Revista de Investigación de Física (Lima, Peru), **7**, 2 (2004).